

Advanced modulation formats for 400-Gbps short-reach optical inter-connection

Xiaogeng Xu,¹ Enbo Zhou,¹ Gordon Ning Liu,¹ Tianjian Zuo,¹ Qiwen Zhong,¹ Liang Zhang,¹ Yuan Bao,² Xuebing Zhang,² Jianping Li² and Zhaohui Li^{2,*}

¹Transmission Technology Research Department, Huawei Technologies Co., Ltd., Shenzhen, China

²Institute of Photonics Technology, Jinan University, Guangzhou, Guangdong, 510632, China

*li_zhaohui@hotmail.com

Abstract: Besides the long-haul optical networks covering over thousands of kilometers for backbone transmission, short reach optical networks (SR-ONs) are widely deployed in metro-area for aggregation and accessing. The SR-ONs include the metro optical transport networks (Metro-OTN), optical access networks or other optical inter-connection systems with even shorter distance. As predicted, the growing bandwidth demanding from SR-ONs will be much more than that from the long-haul optical networks in the near future. Besides, there are tremendous amounts of optical terminals and end-users in SR-ONs compared with the long-haul transmission systems and thus will induce large cost and huge energy consumption. So, the power and cost efficiency should be the key consideration for SR-ONs besides the transmission performance. To improve the power and cost efficiency in SR-ONs, advanced modulations and detection techniques based on low power, low cost and integrated optical modulators should be utilized. In this paper, different advanced modulation formats have been discussed. 56Gbps PAM4, 112Gbps poly-binary and 100Gbps DMT that can be used to realize 400-Gbps SR-ONs for different applications have also been demonstrated respectively. In addition, low-cost and low-power opto-electronic components suitable for SR-ONs, the impairments induced by all kinds of defects and bandwidth limitation of opto-electronic components and the corresponding compensation techniques based on DSP algorithms have also been discussed in the experiments.

©2015 Optical Society of America

OCIS codes: (060.2330) Fiber optics communications; (060.4080) Modulation; (060.4510) Optical communications.

References and links

1. S. J. Savory, G. Gavioli, R. I. Killey, and P. Bayvel, "Electronic compensation of chromatic dispersion using a digital coherent receiver," *Opt. Express* **15**(5), 2120–2126 (2007).
2. C. R. S. Fludger, T. Duthel, D. van den Borne, C. Schullien, E.-D. Schmidt, T. Wuth, J. Geyer, E. de Man, G.-D. Khoe, and H. de Waardt, "Coherent equalization and POLMUX-RZ-DQPSK for robust 100-GE transmission," *J. Lightwave Technol.* **26**(1), 64–72 (2008).
3. X. Liu, S. Chandrasekhar, B. Zhu, P. J. Winzer, A. H. Gnauck, and D. W. Peckham, "448-Gb/s reduced-guard interval CO-OFDM transmission over 2000 km of ultra-large-area fiber and five 80-GHz-grid ROADMs," *J. Lightwave Technol.* **29**(4), 483–490 (2011).
4. Metro network traffic growth: an architecture impact study," strategic white paper from Bell Labs.
5. W. Vereecken, W. V. Heddeghem, M. Deruyck, B. Puype, B. Lannoo, W. Joseph, D. Colle, L. Martensand, and P. Demeester, "Power consumption in tele-communication networks: overview and reduction strategies," *IEEE Commun. Mag.* **49**(6), 62–69 (2011).
6. M. P. I. Dias and E. Wong, "Sleep/doze controlled dynamic bandwidth allocation algorithms for energy-efficient passive optical networks," *Opt. Express* **21**(8), 9931–9946 (2013).
7. A. R. Dhaini, P.-H. Ho, and G. Shen, "Toward green next generation passive optical networks," *IEEE Commun. Mag.* **49**(11), 94–101 (2011).
8. P. Cao, X. Hu, Z. Zhuang, L. Zhang, Q. Chang, Q. Yang, R. Hu, and Y. Su, "Power margin improvement for OFDMA-PON using hierarchical modulation," *Opt. Express* **21**(7), 8261–8268 (2013).

9. X. Dong, T. El-Gorashi, and J. M. H. Elmirghani, "On the energy efficiency of physical topology design for IP over WDM networks," *J. Lightwave Technol.* **30**(12), 1931–1942 (2012).
10. I. Cerutti, P. G. Raponi, N. Andriolli, P. Castoldi, and O. Liboiron-Ladouceur, "Designing energy-efficient data center networks using space-time optical inter-connection architectures," *IEEE J. Sel. Top. Quantum Electron.* **19**(2), 203–210 (2013).
11. B. Schrenk, F. B. Bo, J. Bauwelinck, J. Prat, and J. A. Lazaro, "Energy-efficient optical access networks supported by a noise-powered extender box," *IEEE J. Sel. Top. Quantum Electron.* **17**(2), 480–488 (2011).
12. E. Wong, M. Mueller, M. P. I. Dias, C. A. Chan, and M. C. Amann, "Energy-efficiency of optical network units with vertical-cavity surface-emitting lasers," *Opt. Express* **20**(14), 14960–14970 (2012).
13. D.-Z. Hsu, C.-C. Wei, and H.-Y. Chen, "A 40-Gbps OFDM LR-PON system over 100-km fiber employing an economical 10-GHz-based transceiver," in *Proc. OFC (2012)*, OW4B.2.
14. J. L. Wei, J. D. Ingham, D. G. Cunningham, R. V. Penty, and I. H. White, "Performance and power dissipation comparisons between 28Gb/s NRZ, PAM, CAP and optical OFDM systems for data communication applications," *J. Lightwave Technol.* **30**(20), 3273–3280 (2012).
15. Y. Bao, Z. Li, J. Li, X. Feng, B. O. Guan, and G. Li, "Nonlinearity mitigation for high-speed optical OFDM transmitters using digital pre-distortion," *Opt. Express* **21**(6), 7354–7361 (2013).
16. S. H. Han and J. H. Lee, "Modulation, coding and signal processing for wireless communications—an overview of peak-to-average power ratio reduction techniques for multicarrier transmission," *IEEE Wireless Commun. Mag.* **12**(2), 56–65 (2005).
17. D. Kim and G. L. Stüber, "Clipping noise mitigation for OFDM by decision-aided reconstruction," *IEEE Commun. Lett.* **3**(1), 4–6 (1999).
18. L. Ding, Z. Ma, D. R. Morgan, M. Zierdt, and G. Tong Zhou, "Compensation of frequency-dependent gain/phase imbalance in pre-distortion linearization systems," *IEEE Trans. on Circuits Syst. I. Reg. Papers* **55**(1), 390–397 (2008).
19. D. R. Morgan, Z. Ma, J. Kim, M. G. Zierdt, and J. Pastalan, "A generalized memory polynomial model for digital predistortion of RF power amplifiers," *IEEE Trans. Signal Process.* **54**(10), 3852–3860 (2006).
20. A. Lender, "Correlative digital communication techniques," *IEEE Trans. Commun. Technol.* **12**(4), 128–135 (1964).
21. R. Howson, "An analysis of the capabilities of polybinary data transmission," *IEEE Trans. Commun. Technol.* **13**(3), 312–319 (1965).
22. S. Walklin and J. Conradi, "Multilevel signaling for increasing the reach of 10 Gb/s lightwave systems," *J. Lightwave Technol.* **17**(11), 2235–2248 (1999).
23. L. F. Suhr, "112-Gbit/s x 4 Lane Polybinary 4-PAM for 400G Base," in *Proc. ECOC (2014)*, Tu 4.3.2.
24. L. Zhang, Q. Zhang, T. Zuo, E. Zhou, G. N. Liu, and X. Xu, "C-band 100-Gb/s optical IM-DD transmission over 80km SMF without CD compensation enabled by SSB-DMT," Submitted to *Proc. OFC (2015)*.
25. Q. Zhang, Y. Fang, E. Zhou, T. Zuo, L. Zhang, G. N. Liu, and X. Xu, "C-band 56Gbps transmission over 80km single mode fiber without chromatic dispersion compensation by using intensity-modulation direct-detection," in *Proc. ECOC (2014)*, P.5.19.

1. Introductions

The telecom optical networks can be mainly divided into three categories: core, metro and access networks. Optical core networks, also with the backbone networks, are connecting between the cities or nations, based on long-haul (>100km) optical transmission systems. The Metro-OTNs are deployed in metropolitan regions between the core and access networks. The optical access networks (OANs) are called "last one mile" to internet users. Generally, the user data are first transmitted into the OAN, aggregated into Metro-OTN, finally packaged and uploaded into the core networks [1–3].

In 2012, study from the Bell Labs indicates that total metro traffic will increase 560 percent from 2013 to 2017. IP video, data center (DC) and cloud traffic are the largest drivers for growth. The Bell Labs study forecasts that traffic derived from video will increase about 720 percent, while the DC traffic will increase more than 440 percent. The combined growth rate from the video and DC in metro will reach about 560 percent by 2017 and is about two times faster than traffic in backbone network. This faster growth rate will require scaling of network nodes and links in the optics domains of metro network [4].

Furthermore, current traffic distribution is also changing from 2013 to 2017. By 2017, 75 percent of total metro traffic will be terminated within the metro network, while only 2 percent of traffic needs to traverse through the backbone network [4].

Since the internet traffic growth in metro network is much larger than that in backbone network and most of the traffic terminate within the metro network, huge energy and cost in

metro network are increased significantly [4]. Besides, due to the large amounts of power-on optical nodes and end-users in Metro-OTNs and OANs, the energy consumption and cost of short reach (<100km) optical networks (SR-ONs), are much more sensitive than those in backbone networks. So, the power and cost efficiency should be the key consideration for SR-ONs besides the transmission performance. Among these smart network technologies, the power-saving, cost-efficiency strategies, spectrum-efficient and soft defined network (SDN) techniques are attracting more and more attentions.

In recent years, various technologies in software and hardware layers have been proposed to improve the energy efficiency, including dynamic topology optimization for network topologies, adaptive link rate for wired access networks and hybrid hierarchical base station deployment for wireless access networks etc [5]. Recently, there have been many studies on how to improve the energy-efficiency of the SR-ONs, such as [6–12]. In [6,7], sleep/doze strategies of optical network units (ONUs) are employed for the energy-efficient passive optical networks (PONs). The bandwidth can be allocated dynamically to fit the traffic transmission. In [8], hierarchical modulation is proposed to improve the power margin of ONUs far from the optical line terminal (OLT). Energy-efficient physical topologies for the optical transport networks (e.g. Metro-OTN) are investigated in [9]. These techniques are based on the software definition protocols. Space-time inter-connection architecture, which is based on low power space switches composed of semiconductor optical amplifiers (SOAs), is proposed for data center networks [10]. Optically noise-powered extender box is proposed to reuse the optical noise as pumping power to extend loss budget and thus reduces the wastage of the optical noise, which still consumes energy [11]. However, these technologies are usually difficult and expensive for implementation.

Alternatively, utilization of low-power and low-cost opto-electronic components is also an important research direction. High spectrum-efficient SR-ONs based on low-power and low-cost integrated modulators, such as electro absorption modulated laser (EML) and vertical-cavity surface-emitting laser (VCSEL), is investigated in recent years. An energy-efficient ONU based on direct modulated VCSEL is demonstrated [12]. Nevertheless, the line rate of VCSELs cannot support for the high speed SR-ON transmission. An EML is an electro-absorption modulator (EAM) monolithically integrated with a distributed feedback (DFB) laser, which are demonstrated in many potential applications in SR-ONs [13]. Compared with conventional LiNbO₃ Mach-Zehnder modulators (MZMs), the integrated optical modulators have a lot of advantages, such as low driven voltage, low energy consumption, cost-efficiency and compact sizes.

Comparing the advantages between deployments in different wavelength range, one would be first aware of that the legacy of the transmission fiber is most deployed with standard single mode fiber (SSMF). As a result, O band has the advantages of dispersion free. However, the number of commercially available wavelength is far less than that in C band. Also, SOAs are the only option in this wavelength range which further limits the delivery distance within 40 km in most of commercial scenarios. In contrast, deployment in C band is benefited from the DWDM technique and low cost optical amplifiers, such as Erbium doped fiber amplifier (EDFA).

The non-return-to-zero (NRZ) maximum likelihood sequence estimation (NRZ-MLSE) modulation technique is already commercially available with moderate tolerance to residual chromatic dispersion (CD). Recent report on pulse amplitude modulation (PAM4)-MLSE can improve the spectrum efficiency (SE), but the tolerance to residual CD drops dramatically, which will limit its implementation in very short distance or in O band. Discrete multi-tone (DMT) is a variant of orthogonal frequency division multiplexing (OFDM) modulation format. With flexible power and bit loading technique, it has strong tolerance to residual CD and can make full use of bandwidth of the system. However, its performance is not comparable to single wavelength system if the CD along the fiber link can be well managed [14].

At the receiver side, the CD induced impairment is no longer a big issue in coherent detection. However, the cost of coherent detection is extremely too high to afford for SR-ON system. It would be used only if new platforms cut down the cost efficiently in future. On the other hand, non-coherent detection with only a single PIN or avalanche photodiode (APD) receiver is very attractive due to low cost.

Considering the cost and power efficiency, we have to choose the low-cost and low power opto-electronic components with nonlinear effect, chirp effect, bandwidth limitation and other impairments. As a result, digital signal processing (DSP) has to be introduced to compensate these impairments and improve the performance degraded due to low-cost and low-power opto-electronic components, such as clipping, pre-emphasis, digital pre-distortion (DPD) algorithm and other DSP algorithms to mitigate the I/Q imbalance, peak-to-average power ratio (PAPR), signal-to-signal beat interference (SSBI), CD induced power penalty [15–18].

In this paper, we discuss advanced modulation formats, such as PAM, poly-binary and DMT that can be used to realize 400-Gbps SR-ONs for different applications. We also pay attention to the low-cost and low-power opto-electronic components suitable for SR-ONs, the impairments induced by all kinds of defects and bandwidth limitation of opto-electronic components and the corresponding compensation techniques based on DSP algorithms.

2. Advanced Modulation Formats for 400Gbps SR-ONs

2.1 PAM4 system for 8x50Gbps 400GE Optical Interface up to 10km

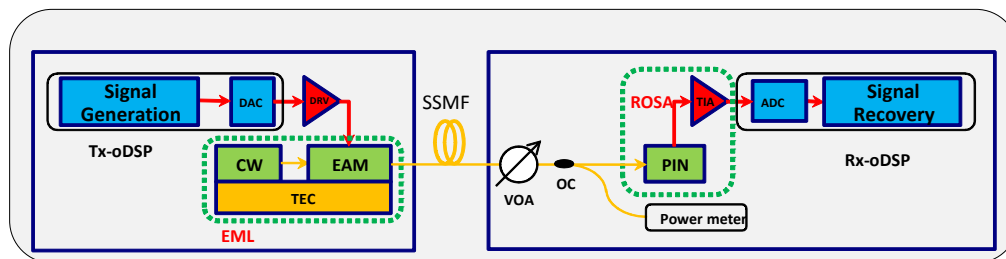


Fig. 1. Experimental setup for PAM4 system.

The experimental setup for PAM4 system is shown in Fig. 1. The 56Gbps PAM4 signal with 400M symbols in pseudo random binary sequence (PRBS) with $2^{15} - 1$ in length is generated by a SHF 12103A signal generator and fed into SHF 3-bits digital to analog convertor (DAC) PAM4 transmitter. After electrically amplified by a linear driver, the signal is sent to a CIP electro-absorption modulated laser (EML) at 1320 nm with 22-GHz at 3-dB bandwidth. A thermoelectric cooler (TEC) is used to stabilize the EML. At receiver, a variable optical attenuator (VOA) is used to change the incident optical power. A 3/97 optical coupler is used to timely monitor the optical power launched into the receiver optical sub-assembly (ROSA). The ROSA with a PIN diode and a linear trans-impedance amplifier (TIA) is used to detect optical signal. After sampled by a digital oscilloscope with 80GSa/s, the received electrical signal is collected and processed by DSP off-line. 10-km SSMF with zero dispersion wavelength (ZDW) of approximately 1310nm and maximum dispersion slope of $0.092\text{ps/nm}^2 \cdot \text{km}$ is used in transmission experiment. The fiber loss is 0.39dB/km measured at 1320nm.

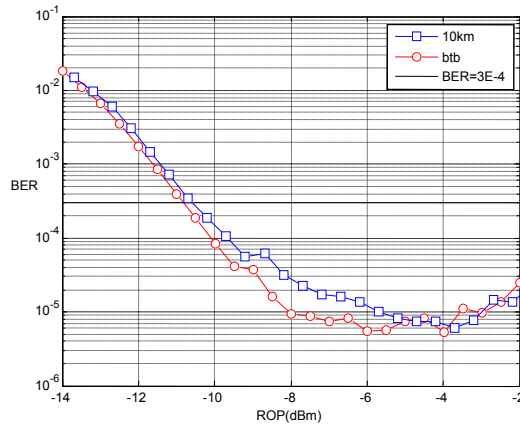


Fig. 2. 56-Gbps PAM 4 based on 1320nm EML/PIN PAM4 experiment results for B2B and 10-km SSMF transmission.

Due to the limitation in slow carrier lifetime of EML, pattern effect will induce the inter-symbol interference (ISI) in system. As a result, a linear equalizer with 17 taps is used in DSP at receiver to compensate such impairment. Meanwhile, in order to make the EML work around the linear region, an approximately 4-dB loss in extinction ratio (ER) is observed in the experiment.

The power penalty induced by fiber CD is approximately 0.2dB (CD = 8 ps/nm/km). It is shown in Fig. 2 that the sensitivity is approximately -10.81dBm at the FEC threshold of bit-error-rate (BER) equal to 3×10^{-4} . The 7% overhead can reach such a BER level with low complexity in realization. After 10-km transmission, the measured power penalty is about 0.23dB at the FEC threshold of BER equal to 3×10^{-4} by using 100G-KP4, RS(544,514).

It can be concluded that such low sensitivity is only suitable for transmission within 10km. However, one can expect even longer transmission or larger dynamic range if the nonlinear equalizer is used in DSP and EML also works in nonlinear region. An even more complex FEC is another option. A trade-off between the complexity in realization and performance should be carefully optimized in product's level design.

2.2 112Gbps IM-DD poly-binary modulation format for 400Gbps SR-ONs systems

To achieve even lower cost per bit, 100Gbps per lane is highly desired and discussed recently. We know that PAM4 signal requires a baud-rate of 56Gbaud to achieve 112Gbps. In contrast, poly-binary signal is a partial response modulation scheme [19–22], where the spectra occupied can be reduced to half of the system baud-rate. Here we introduce some controlled ISI to each bit according to the poly-binary signal. The poly-binary signal can be directly generated using the logic coding in the experiment. Therefore, pre-emphasis at transmitter side is not mandatory. The formula of coding and decoding for poly-binary signaling is shown in Eqs. (1)–(3), where a_k is the original bit sequence, b_k is the pre-coded sequence, and c_k is the generated seven level signal. It is possible to recover the original binary sequence from independent decisions on c_k after this simple coding.

$$b_k = a_k - b_{k-1} \text{ mod } 4 \quad (1)$$

$$c_k = b_k + b_{k-1} \quad (2)$$

$$a_k = c_k \text{ mod } 4 \quad (3)$$

In previous report [23], the Eq. (2) was realized by using a low pass filter with a 3-dB cut-off bandwidth around quarter of the original signal. The main optimization in this experiment is to utilize the low-pass digital filter at receiver. The advantage of this method is the end to end system analogue bandwidth can also contribute to the effect of narrow band filtering, which will improve the system performance [22]. A digital equalizer at the receiver side uses c_k as the training sequence in the preambles. Furthermore, the transmitter generates conventional PAM4 signal would be highly compatible to public standard, such as IEEE P802.3bj.

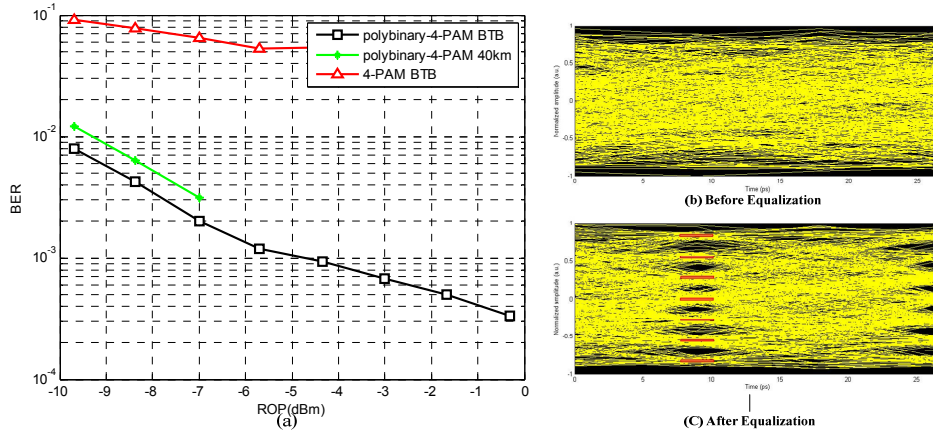


Fig. 3. (a) BER curve of the 112Gbps IM-DD poly-binary systems Eye-diagram of the signal (b) before and (c) after equalizer.

Figure 3(a) shows the BER curves for different link configurations including BTB and 40-km fiber transmission. For fair comparison, the BER of a conventional PAM4 worked with the same linear equalizer with 11-taps and the same length of the training sequence is also included in the Fig. 3(a) performed on the same test-bed. It shows that the sensitivity of poly-binary PAM4 obtained is around -8.5dBm at BER threshold of 4.5×10^{-3} for BTB case. In addition, the complexity and performance can be optimized by using two-dimensional BCH codes. A transmission penalty of 1.5dB is observed. The BER curve for conventional PAM4 is above the FEC limit. In case of 400Gbit/s client side transmission links, the sensitivity allows the poly-binary PAM4 to become a potential solution for the long reach scenarios of 400GE. Figure 3(b) and Fig. 3(c) show the eye-diagram of the signal before and after the equalization, respectively.

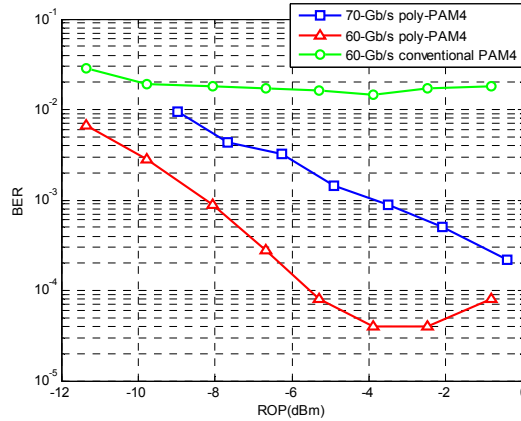


Fig. 4. BER curve of 10-GHz EML/PIN-ROSA based IM-DD poly-binary systems.

For further investigation the influence of low cost 10-GHz optical components on poly-binary, we carry out the experiment of poly-binary PAM4 using 10GHz EML and 10GHz PIN-ROSA. It is shown in Fig. 4 that the sensitivity of approximately -10.65dBm and -7.17dBm is obtained for 60Gbps and 70Gbps poly-binary PAM4 signals respectively. In contrast, 60Gbps conventional PAM4 is always above the FEC threshold.

2.3 100-Gbps IM-DD OFDM over 80-km SMF enabled by SSB-DMT

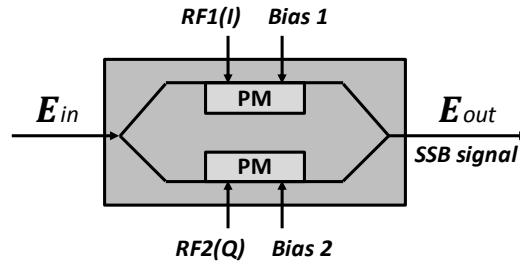


Fig. 5. Principles of the generation of optical SSB signal based on a DD-MZM.

The previous client side solution is very attractive in low cost and large capacity per lane. However, commercially available wavelength in O band is limited, even larger capacity per fiber link can be only realized in C-band where more than 80 channels in ITUT-50-GHz grid are defined. However, the CD induced power penalty in C-band is a big issue in direct direction and the cost will be dramatically increased if IQ modulator is used. A solution with low cost platform for 100Gbps per wavelength is highly desired to further decrease cost per bit and improve spectral efficiency. In this section, a novel single side band (SSB)-DMT solution based on IM-DD with strong tolerance to 80-km residual CD is experimentally demonstrated [24].

Figure 5 shows the principle to generate single optical SSB modulation based on a DD-MZM, which is comprised of two parallel phase modulators (PM). For a complex signal $Txwave(t) = I(t) + j*Q(t)$, the real and imaginary components are used to drive the two PMs with a bias difference of $V_\pi / 2$. The output of the DD-MZM can be defined by Eq. (4),

$$E_{out} = \frac{\sqrt{2}}{2} E_{in} * \left\{ e^{j*\left[\frac{\pi}{V_\pi} I(t) - \frac{\pi}{2}\right]} + e^{j*\left[\frac{\pi}{V_\pi} Q(t)\right]} \right\} = \frac{\sqrt{2}}{2} E_{in} * \left\{ -j * e^{j*\left[\frac{\pi}{V_\pi} I(t)\right]} + e^{j*\left[\frac{\pi}{V_\pi} Q(t)\right]} \right\} \quad (4)$$

When the $I(t)$ and $Q(t)$ are small signals, thus Eq. (4) can be approximated as Eq. (5),

$$E \approx \frac{\sqrt{2}}{2} E_{in} * \left\{ -j \left[1 + j * \frac{\pi}{V_{\pi}} I(t) \right] + \left[1 + j * \frac{\pi}{V_{\pi}} Q(t) \right] \right\} \approx \frac{\sqrt{2}}{2} E_{in} * \left\{ \frac{\pi}{V_{\pi}} * [I(t) + j * Q(t)] + 1 - j \right\} \quad (5)$$

The electrical complex signal $Txwave(t) = I(t) + j * Q(t)$ is linearly converted to optical domain based on Eq. (5). Thus, an optical SSB signal can be obtained if the real and imaginary components of an electrical SSB are used to driven a DD-MZM biased at the quadruple point. Although optical SSB signal can be generated by IQ-MZM, the proposed DD-MZM based method has the advantages of low cost, simple configuration and easy implementation.

The experimental setup of SSB-DMT system is shown in Fig. 6. The DMT signal is generated offline. The binary bits are mapped to subcarriers according to the bit loading results. In order to generate single electrical SSB signal, only the first-half subcarriers are loaded with data, while the others are set to zero, thus the real part I and imaginary part Q of the 1024-point IFFT output are Hilbert pair. A cyclic prefix (CP) of 32 samples is added to alleviate the ISI incurred by fiber CD. After the parallel to serial (P/S) conversion, the clipping process is utilized to reduce the PAPR, which is a critical parameter of DMT system. Then I and Q data are transmitted through 2 DACs with a 3-dB bandwidth of approximately 12GHz and a sample rate of 64Gbps. After that, the electrical signal is amplified to a proper value (peak-to-peak at ~800mV). A laser at 1550nm is fed into a DD-MZM with a half-voltage of 3.5V and a bandwidth of 22GHz. When the DD-MZM is biased at quadruple point, an optical SSB-DMT signal is achieved.

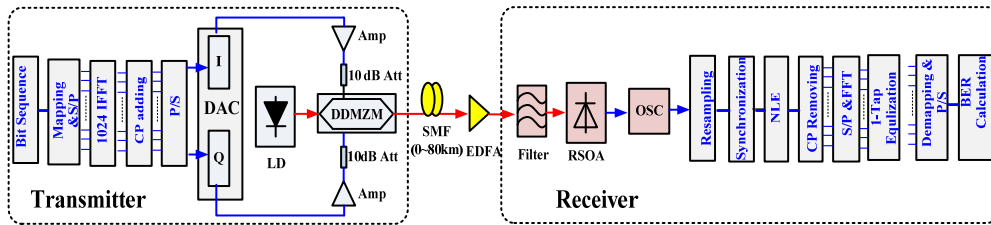


Fig. 6. Experimental setup of the proposed DD-MZM-based SSB-DMT system.

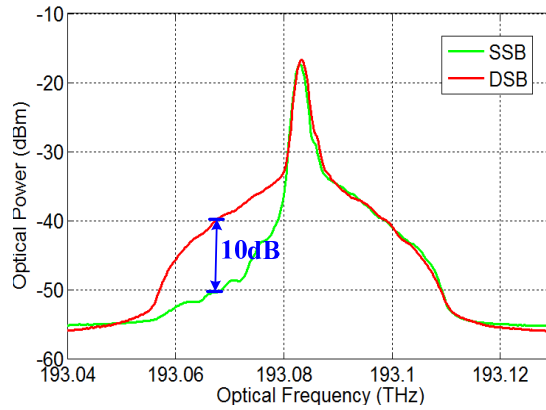


Fig. 7. Optical spectra of SSB-DMT and DSB-DMT signals.

The optical spectrum of the SSB-DMT signal is shown in Fig. 7, where the suppression ratio is higher than 10dB compared with the double side band (DSB)-DMT signal. In transmission, modulated signal with 3-dBm incident optical power over 80-km SSMF is tested.

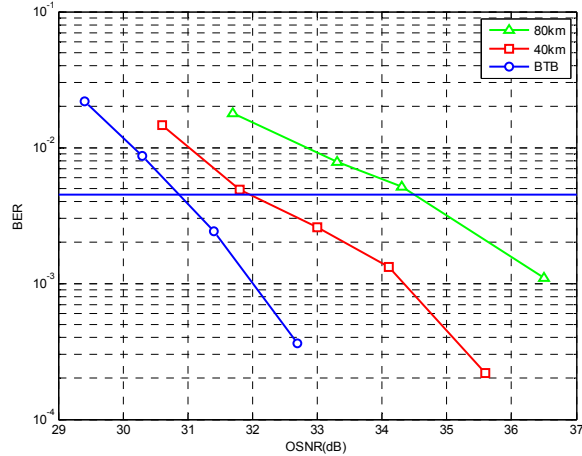


Fig. 8. BER performances of 100-Gbps SSB-DMT system.

At the receiver side, the optical signal is amplified by an EDFA and a following optical band-pass filter (BPF) is used to filter out the amplified spontaneous emission (ASE) noise outside the pass-band. The center wavelength of optical filter is slightly detuned to further suppress the left band of the SSB-DMT signal. A ROSA is used to convert the optical signal to analog electrical signal. A real-time oscilloscope (OSC) is employed to capture the SSB-DMT signal at a sampling rate of 80Gbps and offline DSP processing is implemented to demodulate the signal. Nonlinearity estimation & compensation (NLE) algorithm is used to mitigate system nonlinearities induced by direct-detection process and nonlinearity from the optical modulator. Meanwhile, a 1-tap equalization compensates the linear distortions of the system. After the compensations and inverse processing, the constellations and BER of the system can be obtained.

In the experiment, the DMT signal of QPSK modulation for all subcarriers with an equal power is transmitted for SNR testing. The SNR results after 80-km SMF transmission is used for bit and power allocation through modified Chow's algorithm [25].

The BER versus OSNR curves are shown in Fig. 8. The required OSNR for BER equal to 4.5×10^{-3} are 30.9 dB, 32.2 dB and 34.2 dB for the cases of BTB, 40-km and 80-km SMF transmissions, respectively.

3. Conclusion

In this paper, we discuss the low-cost and low-power opto-electronic components suitable for SR-ONs, the impairments induced by all kinds of defects and bandwidth limitation of the opto-electronic components and the corresponding compensation techniques based on DSP algorithms. We also pay attention to the advanced modulation formats, such as PAM4, poly-binary and DMT that can be used to realize 400-Gbps SR-ONs for different applications and demonstrate 8x50Gbps PAM system over 10km SMF, 112Gbps poly-binary system over 40km SMF and 100Gbps DMT system over 80km SMF, respectively.

Acknowledgments

The authors would like to acknowledge the support of National High Technology 863 Research and Development Program of China (No. 2013AA013300) and (No. 2013AA013403), National Natural Science Foundation of China (NSFC) under Grant (No. 61435006, 61307092) and New Century Excellent Talents in University (NCET-12-0679).